MICHIGAN STATE UNIVERSITY

CYCLOTRON LABORATORY

LIGHT FRAGMENTS FROM $^{14}N + Ag$ COLLISIONS AT 35 MeV/NUCLEON

F. DEÁK, A. KISS, Z. SERES,

A. GALONSKY, L. HEILBRONN, and

H.R. SCHELIN

JUNE 1990

MSUCL-731

MSUCL-731
June, 1990

To be published in Phys... Rev. C.

Light Fragments from ^{14}N + Ag Collisions at 35 MeV/nucleon

F. Deak, A. Kiss
Department of Atomic Physics, Eötvös University
Puskin utca 5-7, H-1088 Budapest, Hungary

Z. Seres
Central Research Institute for Physics
H-1525 Budapest 114, Hungary

A. Galonsky, L. Heilbronn, and H.R. Schelin*
National Superconducting Cyclotron Laboratory
and Department of Physics and Astronomy,
Michigan State University, East Lansing, Michigan 48824-1321

Abstract

Velocity spectra of thirteen different fragment species from ^{6}Li to ^{15}N at seven angles from 15° to 83° and of neutrons in coincidence with them have been determined from ^{14}N + Ag collisions at 35 MeV/nucleon. The velocity spectra of the fragments show contributions from quasi-elastic and deep-inelastic processes. The quasi-elastic part of each spectrum was fitted with an empirical model. For each fragment species, the deep-inelastic part at each of the seven angles was simultaneously fitted with a single moving source. The parameters T for source temperature and E/A, corresponding to source velocity, were approximately independent of fragment species and had average values of 12.8 MeV and 3.9 MeV, respectively. Many coincident neutron spectra were created off-line by selecting gates having various fragment species, angles, and velocity intervals. The neutron spectra at seven or eight angles with a given gate were simultaneously fitted with two moving sources. The source parameters had little dependence on the gate. The average values of T and E/A for one source, an intermediate rapidity source, were 10.4 MeV and 10.7 MeV/nucleon, respectively. The other source, a slowly moving target-like source, had T and E/A in the ranges 2.0-3.6 MeV and 0.1-0.3 MeV/nucleon, respectively. Since neither of these neutron sources has the velocity of the fragment source, the actual origin of the deep-inelastic fragments may be a non-equilibrium process such as the stripping-pickup process.

I. Introduction

The energy and angle distributions of fragments emitted in heavy-ion collisions are a major source of information on the mechanisms of those collisions. When the collision energy/nucleon is near the Fermi energy, fragment velocity spectra[1,2] are, to first approximation, independent of the identity of the colliding nuclei. These spectra are dominated by two components, one from quasi-elastic (QE) reactions and one from deep inelastic (DI) reactions. The QE component is most pronounced at high fragment velocities and small angles. The DI component falls off with fragment velocity and becomes dominant at large angles. The physical origin of fragment production has attracted much recent interest.[1-9]

The QE component results from peripheral collisions.[10-13] In one model[2,11,13] the QE spectra result from a projectile fragmentation into a part that penetrates the target and forms a hot participant zone and a projectile-like spectator part that later picks up material from the expanding hot zone, thus forming a projectile-like fragment.

Interpreting the DI component is more difficult. The DI spectra have been successfully parameterized in the framework of thermally emitting moving sources.[1,14,15] However, the observation of fragments with non-statistical excited-state populations in the ^{14}N + Ag reaction at 35 MeV/nucleon[16] raises a question as to whether these fragments are really produced from hot regions of nuclear matter in thermal equilibrium.

A fast mode of nuclear de-excitation is the emission of nucleons. Nucleons should be emitted whenever there is sufficient excitation energy. This is particularly true of neutrons, and since neutrons leave excited nuclear matter without Coulomb distortion, their energy and angle distributions give the most direct measure of the degree of excitation of their source. It is hard to imagine fragment emission without accompanying neutron emission. Hence, the reaction mechanism with which fragments are produced should have consequences seen in the spectra of coincident neutrons.

The aim of this work is to explore these consequences in new data on inclusive fragment production and on fragment-neutron coincidences in the ^{14}N + Ag reaction at 35 MeV/nucleon. The incident energy is around the Fermi level of the colliding nuclei and well within the region where both mean-field

and two-body dissipation processes should show up.[17] The experiment was planned to provide data in an angular region which allows the investigation of both the QE and DI components.

II. Experimental procedure

The experiment was performed with a beam of 490-MeV $^{14}N^{5+}$ ions from the K500 cyclotron at Michigan State University. Most of the apparatus and techniques used in the present experiment have been discussed in detail elsewhere,[10-12,18] so only the essential features will be described here.

The targets were natural Ag foils of 3.9 and 5.0 mg/cm² areal density. The intensity of the N beam was about $2 \cdot 10^{10}$ ions/s for the coincidence runs and an order of magnitude smaller for the singles runs.

The fragments were detected with ΔE-E silicon telescopes at -15.0°, -31°, -64°, and -83° in the horizontal plane and one at 14° out of this plane directly below the beam axis. In addition, the -31° and -64° telescopes were each surrounded by six other telescopes, resulting in two densely packed arrays of seven telescopes. The telescopes at -15° in-plane and 14° out-of-plane consisted of four (two ΔE and two E) and three (one ΔE and two E) elements, respectively. All other telescopes were built from one ΔE and one E detector. The -83° telescope consisted of 30-μm and 1-mm elements. For the other telescopes the ΔE elements were 75 or 100 μm thick, and the first E elements were 5 mm thick. Where there was a second E detector it was 1 mm thick. The solid angles ranged from 2.3 to 8.7 msr for the 17 different telescopes. In order to reduce the number of small pulses from electrons and X-rays produced in the target, a gold foil of ~10 mg/cm² was placed in front of each telescope. The fragment telescopes were calibrated with α-particle sources and a precision pulse generator. The uncertainty in fragment energy and the energy resolution of the telescopes were about 2% and 1.5 MeV, respectively.[2]

A schematic view of the experimental setup without the fragment telescopes is shown in Fig. 1 of Ref. 18. The neutron detectors consisted of liquid scintillator (NE213 or BICRON 501) in sealed glass cells. Most of the cells had dimensions of about 12.7 cm diameter and 7.6 cm thickness; some were a little smaller. They were positioned in the horizontal plane at -15°, -31°, -64°, and -115° (on the same side of the beam as the telescopes) and at 15°,

31°, 60°, 110° and 160° (on the opposite side). With increasing angle, the distance from the beam spot to the face of a neutron detector was 452, 438, 353, 164 cm for the negative angles and 204, 205, 165, 164, 106 cm for the positive angles. In order to improve the statistical accuracy for fragment-neutron coincidences resulting from sequential decay, that is, when the fragment and the neutron go off in the same direction, clusters of detectors were used at -15°, -31° and -64°, the same angles at which there were Si telescopes. At -15° we mounted three detectors in a triangular arrangement, and at -31° and -64° six detectors tightly encircled a seventh one.

The time resolution of the neutron detectors was about 0.8 nsec for pulses at the ^{60}Co Compton edge. In front of each forward detector (with angles $\leq$ 64°) a 6-mm thick NE102A paddle was placed for the rejection of high energy protons. (Protons which were emitted with energies smaller than 40 MeV were stopped by the material between the target and the neutron detector.) Neutrons were distinguished from gamma rays by pulse shape discrimination using two QDC's.[19] Neutron energy was determined from the time difference between signals from the first element of the fragment telescope and from the neutron detector.[11] Detector efficiency was computed,[10] and attenuation of the neutrons by the material between the target and the detector was taken into account.[11] In-scattering background contributions to the neutron spectra were determined by taking data with shadow bars between the target and the neutron detectors during about half of the run time. The background contribution was typically about 20%.

The data were taken in event mode and the analysis was done off line. In every telescope there was good element separation. For each element a two-dimensional spectrum of particle identification number vs. fragment energy was constructed. This spectrum was sliced into bins 6 MeV wide, and the resulting one-dimensional particle identification spectra were fitted by Gaussians and linear backgrounds for each isotope having a significant intensity. This procedure gave us energy spectra for individual isotopes for each telescope.

In the case of fragment-neutron coincidences, first the fragment isotope identification was performed.[11] Then the neutron time-of-flight was determined using the calculated fragment velocity. After neutron/gamma-ray discrimination was accomplished, neutron time spectra were constructed for each fragment element in bins 7 MeV/nucleon wide. Subtracting the backgrounds and correcting each spectrum for absorption, we determined the differential

neutron cross sections for the telescopes in the horizontal plane for all the Li, Be, B and C fragment element gates.

III. Parameterization of the Fragment Distributions

Fragment velocity (actually velocity squared) spectra were constructed at seven angles from 15° to 83° for isotopes of ^{6}Li, ^{7}Li(+^{8}Be^{20}), ^{7}Be, ^{9}Be, ^{10}Be, ^{10}B, ^{11}B, ^{12}B, ^{11}C, ^{12}C, ^{13}C, ^{14}N, and ^{15}N. A typical set of these spectra, here for ^{6}Li, is displayed in Fig. 1. The spectral shapes for the other isotopes are similar to those in Fig. 1, although the exponential fall-offs at the larger angles are steeper in the spectra for the heavier fragments than for ^{6}Li. The spectra at the four most forward angles in Fig. 1 were fitted with a model having two-components, a quasielastic (QE) component and a deep inelastic (DI) component. The QE component has an empirical prescription.[2] Its strength falls off rapidly with angle and is negligible beyond 57°. For the heavier of our fragments it becomes negligible at angles smaller than 57°, but it is always dominant at 15°. The DI component has the standard parameterization of a hot source moving at 0°. Table I contains the values of the fit parameters--σ, the source strength; T, the source temperature; and E/A, the source velocity (squared and times 1/2). The quality of the fits in Fig. 1 is typical of the fits for the other isotopes.

IV. Neutron-fragment coincidences

As was shown in the previous section and in Refs. 2,10,11 and 13, the fragment angle can serve as a selection trigger for the QE or DI reaction mechanism. Accordingly, most neutrons detected in coincidence with fragments at 15° are emitted in QE processes, while most of those in coincidence with fragments at larger angles come from DI reactions.

The data in Fig. 2 are neutron spectra at +60° gated by the indicated fragments at -15° in a velocity interval corresponding to 14 to 21 MeV/nucleon. Figure 1 shows that this gate with Li fragments contains somewhat more QE than DI. With the heaviest fragments--B,C, and N--the mechanism selected by the gate is almost entirely QE. The main feature of the neutron spectra is that they have two components, a feature observed in

earlier experiments.[10,11,13] In terms of moving thermal sources, the low-energy component originates from a slowly-moving, target-like (TL) source and the high energy component from a hotter, fast or intermediate-rapidity (IR) source.[11,13] The fit parameters for each source were the temperature (T), one-half velocity squared or energy/nucleon (E/A) value, direction, and amplitude or multiplicity. Each solid line in Fig. 2 shows the fit with these sources to a neutron spectrum in Fig. 2 plus neutron spectra at six other angles. For the data with the nitrogen gate the individual contributions from the two sources are also shown. Decomposition of the fits to the other spectra look the same. The quality of the fits to neutron spectra at other angles and with gates for fragments of other velocity intervals is almost as good as in Fig. 2.

As with data from targets of C, Ni and Ho,[13] for the Ag data presented here the temperature and velocity parameter values of the IR source showed no significant trend with particulars of the fragment gate, that is, with fragment species or with fragment velocity interval. The average values and the deviations for the T and E/A parameters are 10.4 ± 1.6 MeV and 11.0 ± 2.1 MeV/nucleon, respectively. For the TL source, however, the values of T and E/A both decreased with increasing fragment velocity, from 3.4 ± 0.3 to 2.4 ± 0.3 MeV for T and from 0.25 ± 0.05 to 0.10 ± 0.05 MeV/nucleon for E/A. The directions of the sources are similar those reported in Refs. 11 and 13.

Unlike the temperature and velocity of the IR source, the multiplicity did depend on the gate; for fragment gates dominated by the QE process multiplicity decreased with increasing fragment mass. The obvious implication of this is that the greater the fragment mass, the smaller the source mass. Source mass (or source mass number) is not a parameter of the thermal model. Additional reaction details are needed to predict source mass. The stripping-pickup model of peripheral collisions[11,13] provides such details. This model assumes that a hot participant source develops in the interaction of an abraded part of the projectile with an approximately equal mass from the target nucleus. This source emits the IR neutrons (and protons). Later the coincident fragment is formed in a decelerating mass pickup from the source by the projectile spectator. Multiplicity should increase with both mass and temperature of the source. However, as the fitting analysis above showed source temperature to be approximately constant, at about 10 MeV, the IR neutron multiplicity should increase linearly with the mass of the IR source. To test for this correlation we plotted, for each fragment gate, multiplicity

(as determined from the fit to the neutron spectra) versus mass (as determined from the fitted value of source velocity and the kinematic consequences[13] of the model). Figure 3 displays such a plot when the gating fragments are at 14° below the beam. A rough linear correlation is apparent. When the gating fragments are at 15° in the horizontal plane (the plane of the neutron detectors), where QE reactions again dominate, a similar correlation exists. Previous analyses of QE reactions from Ni and Ho targets[11,13] also showed this correlation.

The other consequence of the stripping-pickup model, that multiplicity decreases linearly with fragment velocity,[11] has been verified with the present data and with the earlier data as well.

As illustrated in Fig. 1, the fragments at angles $\geq 31°$, especially low energy fragments, originate almost entirely in DI processes. Neutron spectra gated by fragments at these larger angles show contributions from the same two sources found with fragment gates at 15°, viz., IR and TL sources. As an example, Fig. 4 shows neutron spectra at +60° gated by various fragment elements at -31° and in the velocity interval 7-14 MeV/nucleon. The similarity to Fig. 2, where the gate is largely on QE processes, is apparent.

The DI data could, therefore, be parametrized in the framework of two moving sources. Each solid line in Fig. 4 shows the two-source fit to a neutron spectrum in the figure plus spectra at seven other angles, and the fit with the nitrogen gate shows, in addition, the decomposition of the fit into a TL and an IR source. The quality of the fits in Fig. 4 is representative of the quality of the fits to neutron spectra with gates having other fragment velocities and angles. The T and E/A parameters of the IR source had values in the ranges 10.0 ± 1.5 MeV and 10.5 ± 2.0 MeV/nucleon, respectively, independent of the species, velocity, and angle of the gating coincident fragment. With increasing fragment velocity the temperature of the TL source decreased from about 3.6 ± 0.3 MeV to 2.9 ± 0.3 MeV and the velocity parameter decreased from 0.3 ± 0.05 to 0.2 ± 0.05 MeV/nucleon. As was seen with Ni and Ho targets[11,13] the DI neutron multiplicities determined here show no significant change with fragment velocity. For the IR source they scatter between 1.5 and 2.6; for the TL source between 5 and 7 for fragments at 31°, and between 8 and 12 for fragments at 64°.[10]

V. Mechanisms for Fragment Emission

Table I shows that for DI fragment production neither the velocity nor the temperature parameter deviates much from isotope to isotope, although there is a slight increase in both values from ^{6}Li to ^{15}N. This similarity suggests that a single mechanism is responsible for the production of most of the DI fragments. A moving source origin would be quite in the spirit of our investigation. And Table I gives the parameter values of such a source. However, there is a physical inconsistency. Looking at Table II, in which the average values of source temperature and velocity parameters are gathered, we see that the temperature of the DI fragment source (12.8 ± 0.9 MeV) is about the same as the temperature of the IR neutron sources, but its velocity parameter, E/A, has a value (3.9 ± 0.5 MeV/nucleon) much lower than E/A of the IR neutron sources. The inconsistency is that it is hard to imagine a hot source that emits fragments but not neutrons. The neutron analyses, while producing sources of about the same temperature, had them moving much faster, at approximately half the beam velocity. In fitting the neutron spectra there was no indication of a source having E/A around 4 MeV/nucleon. Perhaps the fragments are emitted from the IR source, but only (or mostly) after neutron emission and after the source has slowed down. Another possibility is that a thermal-source fit to the DI fragment data, while mathematically valid, does not represent a physically real equilibrium emission.

The stripping-pickup model is a non-equilibrium model. It gives a qualitative explanation of the shape of the QE fragment spectrum. The peak in such a spectrum, the 15° spectrum of Fig. 1, for example, is just below the velocity of the projectile, and it has a low-velocity tail. In the model, the projectile splits into a part that creates a hot zone in the target and a spectator. The hot zone emits neutrons, protons, etc. and then the spectator picks up some nucleons in a decelerating interaction with the hot zone and becomes the fragment. The more nucleons picked up, the more deceleration and (since the single-nucleon pick-up probability is small) the smaller the probability. Hence, the low-velocity tail. In this model the fragment, as suggested by Borderie et al.,[21] is the final product of the DI collision.

By symmetry of nucleus-nucleus collisions in the CM system, we can imagine reactions to occur in which the target splits and, as in projectile splitting, the spectator part, after some interaction, becomes the fragment. In this case, however, spectators that interact the least are left almost at rest in the laboratory. Spectator interactions that pick up several nucleons are less probable, but the greater interaction drags them along with the forward-moving

hot zone, imparting a higher velocity in the laboratory. Thus arises the decreasing, almost exponentially-falling, DI spectrum.

Another observation explained by this model is that the DI fragments are more isotropically distributed within the forward hemisphere than are the QE fragments--a simple consequence of the kinematics of the model. The model also predicts that the internal excitation of the fragment should depend on the velocity of the fragment. In this picture the DI fragments with the lower velocities are those that interacted less with the hot zone. The lower-velocity DI fragments would, therefore, be colder than the more energetic ones. (The opposite would be true of QE fragments.) Just such an effect has been reported in ^{14}N + Au collisions at 35 MeV/nucleon[22] and in ^{16}O + Ag and ^{32}S + Ag collisions at 30 MeV/nucleon.[9] A measurement specifically on this effect for the ^{14}N + Ag reaction at 35 MeV/nucleon[12] qualitatively verified the velocity dependence of fragment excitation energy for the QE fragments but did not go to low enough velocities with good enough statistical accuracy to provide a test of the model for the DI fragments. We repeat that the above stripping-pickup model is a non-equilibrium model of fragment emission. Evidence for excited fragments with non-equilibrium state populations[16] was recently found in the same system as ours, ^{14}N + Ag at E/A = 35 MeV. The finding of non-equilibrium is in agreement with that feature of our model.

Support of the Hungarian Academy of Sciences and of the U.S. National Science Founndation under Grants INT-86-17683 and PHY-86-11210 is gratefully acknowledged.

*While on leave from Centro Tecnico Aerospacial and State of Sao Paulo Foundation for Support of Research (FAPESP) Brazil.

References

1. B.V. Jacak, G.D. Westfall, G.M. Crawley, D. Fox, C.K. Gelbke, L.H. Harwood, B.E. Hasselquist, W.G. Lynch, D.K. Scott, H. Stöcker, M.B. Tsang, G. Buchwald, and T.J.M. Symons, Phys. Rev. C **35**, 1751 (1987)

2. A. Kiss, F. Deák, Z. Seres, G. Caskey, A. Galonsky, B. Remington, and L. Heilbronn, Nucl. Phys. **A499**, 131 (1989)

3. D.E. Fields, K. Kwiatkowsky, D. Bonser, R.V. Viola, V.E. Viola, W.G. Lynch, J. Pochodzalla, M.B. Tsang, C.K. Gelbke, D.J. Fields, and S.M. Austin, Phys. Lett. **B220**, 356 (1989)

4. W. Trautmann, K.D. Hildebrand, U. Lynen, W.F.J. Müller, H.J. Rabe, H. Sann, H. Stelzer, R. Trockel, R. Wada, N. Brummund, R. Glasow, K.H. Kampert, R. Santo, E.M. Eckert, J. Pochodzalla, I. Bock, D. Pelte, Nucl. Phys. **A471**, 191c (1987)

5. R. Wada, K.D. Hildebrand, U. Lynen, W.F.J. Müller, H.J. Rabe, H. Sann, H. Stelzer, W. Trautmann, R. Trockel, N. Brummund, R. Glasow, K.H. Kampert, R. Santo, E. Eckert, J. Pochodzalla, I. Bock, and D. Pelte, Phys. Rev. Lett. **58**, 1829 (1987)

6. H.W. Barz, H. Schulz, J.P. Bondorf, J. Lopez, and K. Sneppen, Phys. Lett. **B211**, 10 (1988)

7. Z. Seres, F. Deák, A. Kiss, G. Caskey, A. Galonsky, L. Heilbronn, and B. Remington, Nucl. Phys. **A492**, 315 (1989)

8. V.E. Viola, K. Kwiatkowski, S.J. Yennello, and D.E. Fields, "Equilibrated and non-equilibrated Sources of Complex Fragments from Hot Nuclei", Talk presented at the Symposium on Nuclear Dynamics and Nuclear Disassembly, 197th Meeting of the American Chemical Society, Dallas, TX, April 9-14, 1989

9. R. Wada, D. Fabris, K. Hagel, G. Nebbia, Y. Lou, M. Gonin, J.B. Natowitz, R. Billerey, B. Cheynis, A. Demeyer, D. Drain, D. Gounet, C. Pastor, J. Alarja, A. Giorni, D. Heuer, C. Morand, B. Viano, C. Mazur, C. Ngô, S. Leray, R. Lučas, M. Ribrag, and E. Tomasi, Phys. Rev. C **39**, 497 (1989)

10. B.A. Remington, G. Caskey, A. Galonsky, C.K. Gelbke, L. Heilbronn, J. Heltsley, M.B. Tsang, F. Deák, A. Kiss, Z. Seres, J. Kasagi, and J.J. Kolata, Phys. Rev. C **34**, 1685 (1986)

11. F. Deák, A. Kiss, Z. Seres, G. Caskey, A. Galonsky, C.K. Gelbke, B. Remington, M.B. Tsang, and J.J. Kolata, Nucl. Phys. **A464**, 133 (1987)

12. F. Deák, A. Kiss, Z. Seres, A. Galonsky, C.K. Gelbke, L. Heilbronn, W. Lynch, T. Murakami, H. Schelin, M.B. Tsang, B.A. Remington, and J. Kasagi, Phys. Rev. C **39**, 733 (1989)

13. A. Kiss, F. Deák, Z. Seres, G. Caskey, A. Galonsky, L. Heilbronn, and B. Remington, Phys. Rev. C **38**, 170 (1988)

14. D. Hilscher, Nucl. Phys. **A471**, 77c (1987)

15. C. Bloch, W. Benenson, A.I. Galonsky, E. Kashy, J. Heltsley, L. Heilbronn, M. Lowe, R.J. Radtke, B. Remington, J. Kasagi, D.J. Morrissey, Phys. Rev. C **37**, 2469 (1988)

16. K.T. Nayak, T. Murakami, W.G. Lynch, K. Schwarz, D.J. Fields, C.K. Gelbke, Y.D. Kim, J. Pochodzalla, M.B. Tsang, H.M. Xu, F. Zhu, K. Kwiatkowsky, Phys. Rev. Lett. **62**, 1021 (1989)

17. C.K. Gelbke and D.H. Boal, Prog. Part. Phys. **19**, 37 (1987)

18. H.R. Schelin, A. Galonsky, C.K. Gelbke, L. Heilbronn, W.G. Lynch, T. Murakami, M.B. Tsang, X. Yang, G. Zhang, B.A. Remington, F. Deák, A. Kiss, Z. Seres, and J. Kasagi, Phys. Rev. C **39**, 1827 (1989)

19. J. Heltsley, L. Brandon, A. Galonsky, L. Heilbronn, B.A. Remington, S. Langer, A. Vander Molen, and J. Yurkon, Nucl. Instr. Meth. **A263**, 441 (1988)

20. G.J. Wozniak, H.L. Harney, K.H. Wilcox, and J. Cerny, Phys. Rev. Lett. **28**, 1278 (1972).

21. B. Borderie, M. Montoya, M.F. Rivet, D. Jouan, C. Cabot, H. Fuchs, D. Gardes, H. Gauvin, D. Jacquet, F. Monnet, and F. Hanappe, Phys. Lett. **B205**, 26 (1988).

22. C.B. Chitwood, C.K. Gelbke, J. Pochodzalla, Z. Chen, D.J. Fields, W.G. Lynch, R. Morse, M.B. Tsang, D.H. Boal, and J.C. Shillcock, Phys. Lett. **B172**, 27 (1986)

Table I. Parameters of the moving source fits (σ--production cross section; T--temperature; and E/A--1/2 velocity squared) and the σ-weighted neutron/proton ratios (N/Z) for the deep-inelastic component. The statistical deviations for the parameters are less than 10%, for the N/Z ratios less than 0.02.

Fragment	σ (mbarn)	T (MeV)	E/A (MeV/nucl)	N/Z
^{6}Li	49.9	11.4	3.81	
^{7}Li	79.7	11.6	3.65	1.20
^{7}Be	15.3	12.7	4.66	
^{9}Be	16.5	11.9	3.41	
^{10}Be	9.46	12.4	3.37	1.09
^{10}B	11.6	13.2	3.89	
^{11}B	21.8	12.6	3.44	
^{12}B	3.00	12.8	3.36	1.15
^{11}C	2.65	14.5	4.43	
^{12}C	9.30	13.3	4.17	
^{13}C	6.75	13.1	4.27	1.07
^{14}N	2.17	13.7	4.23	
^{15}N	4.27	12.6	4.34	1.09
Averages		12.8±0.9	3.9±0.5	1.17 (weighted)

Table II.
Average temperature and velocity parameters of the moving sources.

Source for		Temperature (MeV)	E/A (MeV/nucleon)
Neutrons from QE reactions	IR Source	10.4 ± 1.6	11.0 ± 2.1
	TL Source	2.9	0.25
Neutrons from DI reactions	IR Source	10.0 ± 1.5	10.5 ± 2.0
	TL Source	3.3	0.25
Fragments from DI reactions		12.8 ± 0.9	3.9 ± 0.5

Figure Captions

Fig. 1 Spectra of ^{6}Li fragments at (from top to bottom) 15°, 31°, 39°, 57°, 64°, 72°, and 83°. Each dashed line is a fit to the quasi-elastic part; each dot-dashed line is a one-moving-source fit to the remaining (deep-inelastic) part; and each solid line is the sum of the two contributions.

Fig. 2 Neutron spectra at +60° in coincidence with Li, Be, B, C and N fragments at -15° in a velocity interval corresponding to 14 to 21 MeV/nucleon. Each solid line is the result of fitting with two moving sources the spectrum shown plus spectra at six other angles. For the spectrum in coincidence with N fragments we also show the individual contributions from the two sources--a target-like source (dashed line) and an intermediate rapidity source (dot-dashed line) source. The values of fragment angle and fragment velocity interval emphasize quasi-elastic reactions.

Fig. 3 Dependence of neutron multiplicity of the IR (intermediate rapidity) source on the mass number of the source. The coincident fragments of Li, Be, B and C were at 14° out of the plane of the coincident neutrons and in velocity intervals corresponding to 7-14, 14-21, 21-28, 28-35 and (for Li) 35-42 MeV/nucleon. The interval values decrease to the right. The multiplicities were obtained by fitting neutron spectra, and the source masses were computed with the stripping-pickup model.

Fig. 4 Neutron spectra at +60° in coincidence with Li, Be, B, C and N fragments at -31° in a velocity interval corresponding to 7 to 14 MeV/nucleon. Each solid line is the result of fitting with two moving sources the spectrum shown plus spectra at seven other angles. For the spectrum in coincidence with N fragments we also show the individual contributions from the two sources--a target-like source (dashed line) and an intermediate rapidity source (dot-dashed line) source. The values of fragment angle and fragment velocity interval emphasize deep-inelastic reactions.

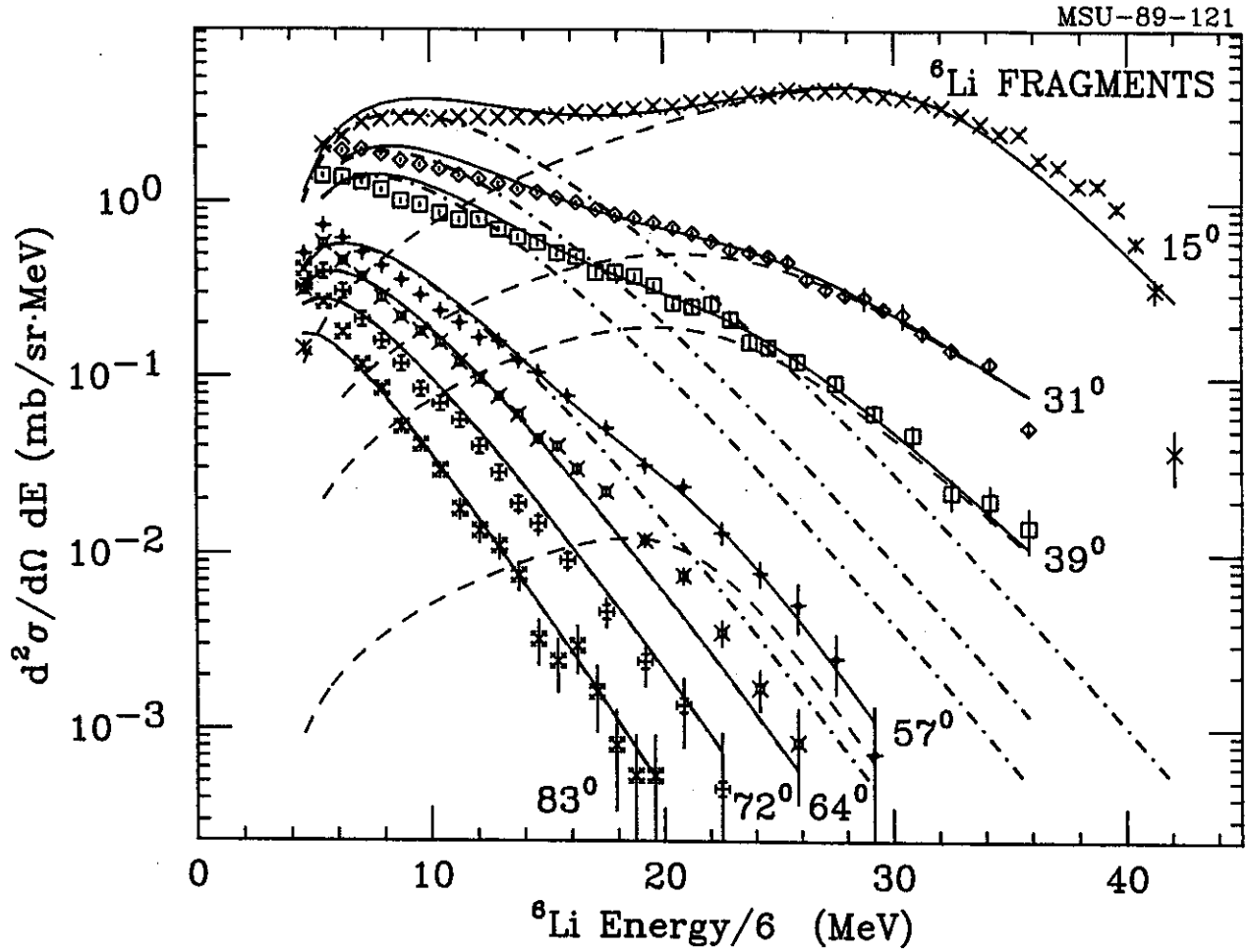
MSU-89-121
^{6}Li FRAGMENTS
15^0
31^0
39^0
57^0
64^0
72^0
83^0
10^0
10^{-1}
10^{-2}
10^{-3}
$d^2\sigma/d\Omega\ dE$ (mb/sr·MeV)
0
10
20
30
40
^{6}Li Energy/6 (MeV)

Fig

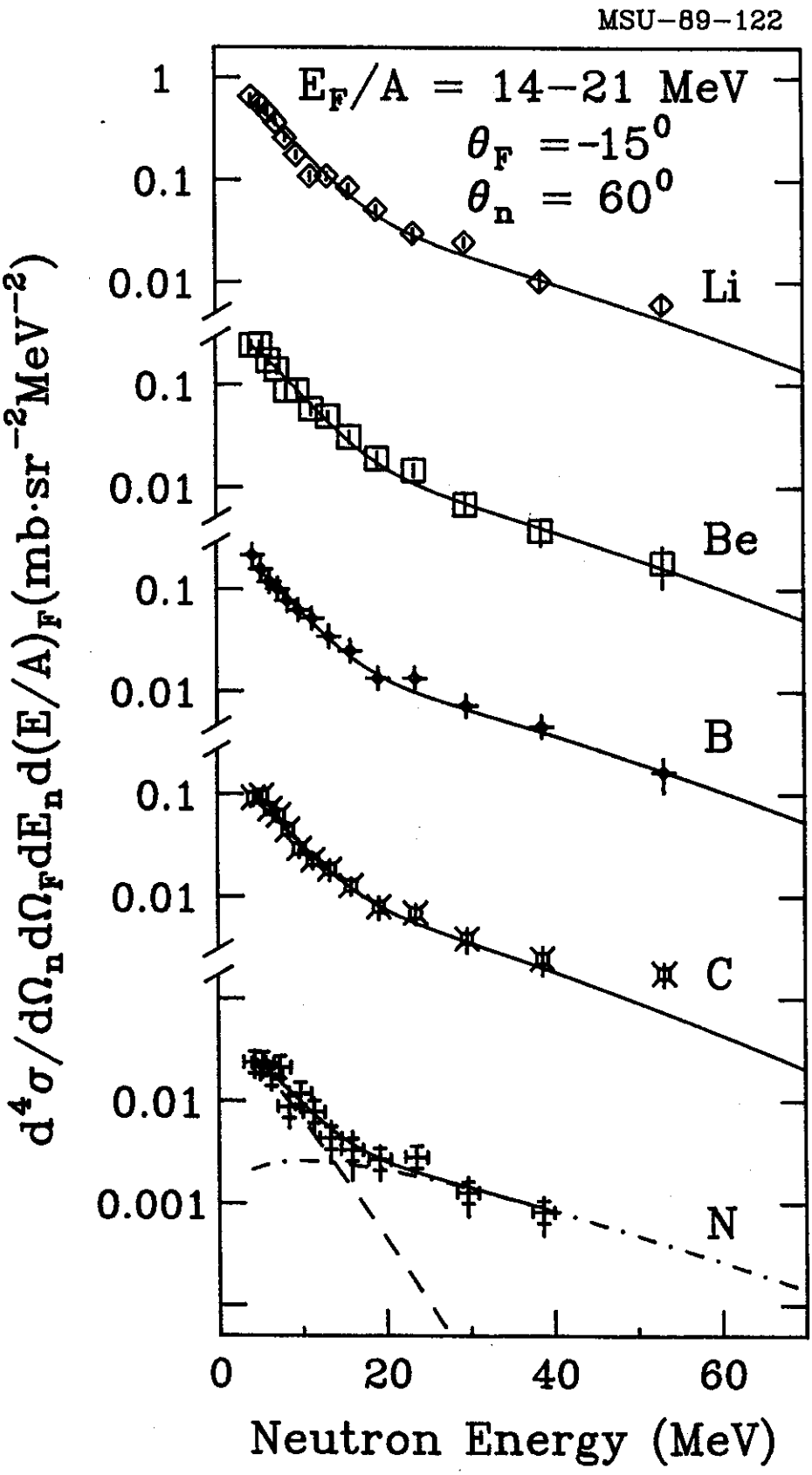
MSU-89-122
E_F/A = 14–21 MeV
θ_F = -15°
θ_n = 60°
Li
Be
B
C
N
1
0.1
0.01
0.1
0.01
0.1
0.01
0.1
0.01
0.001
0
20
40
60
Neutron Energy (MeV)
$d^4\sigma/d\Omega_n d\Omega_F dE_n d(E/A)_F$ (mb·sr^{-2}MeV^{-2})

FIG 2

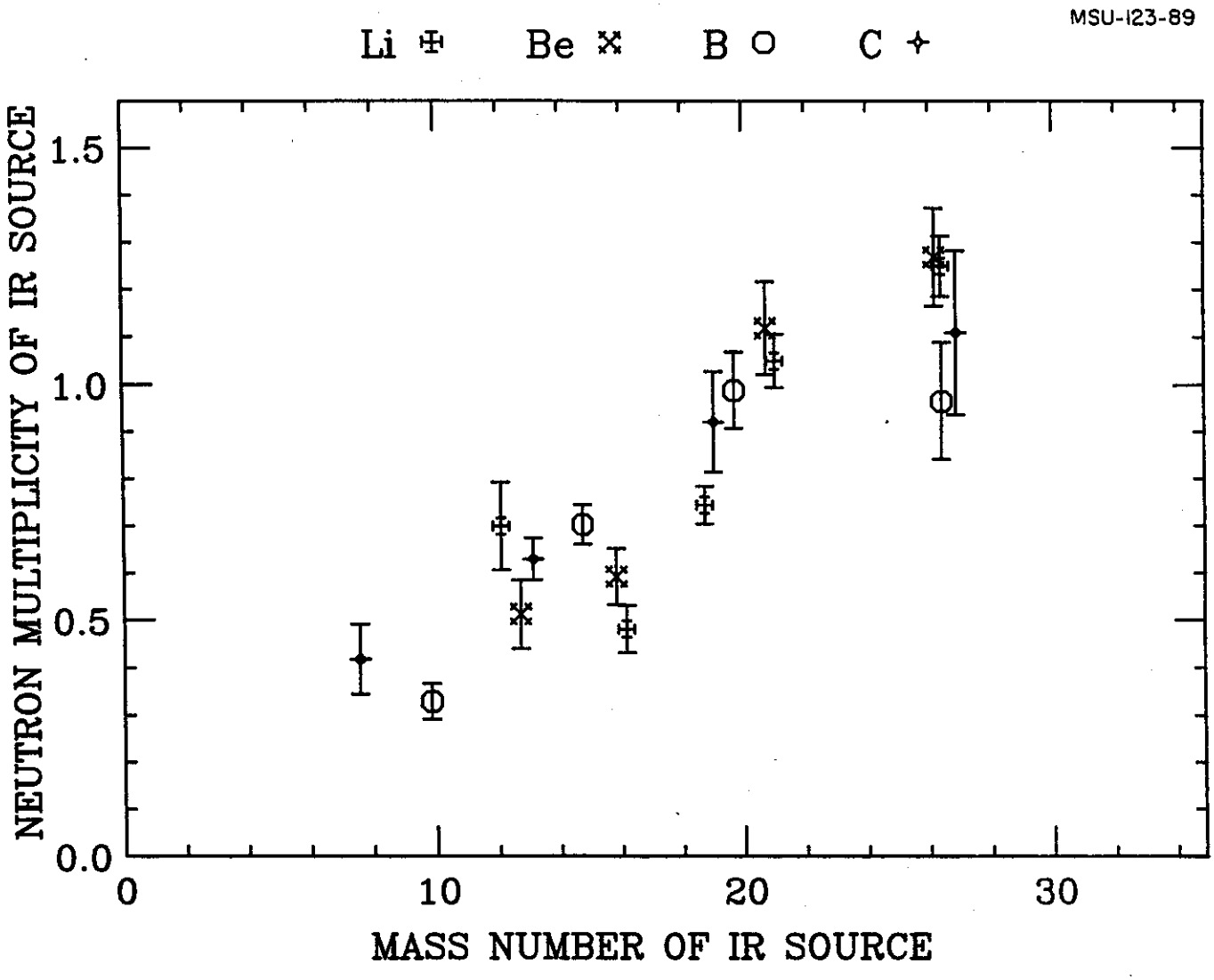
MSU-123-89
Li
Be
B
C
NEUTRON MULTIPLICITY OF IR SOURCE
1.5
1.0
0.5
0.0
0
10
20
30
MASS NUMBER OF IR SOURCE

FIG. 3

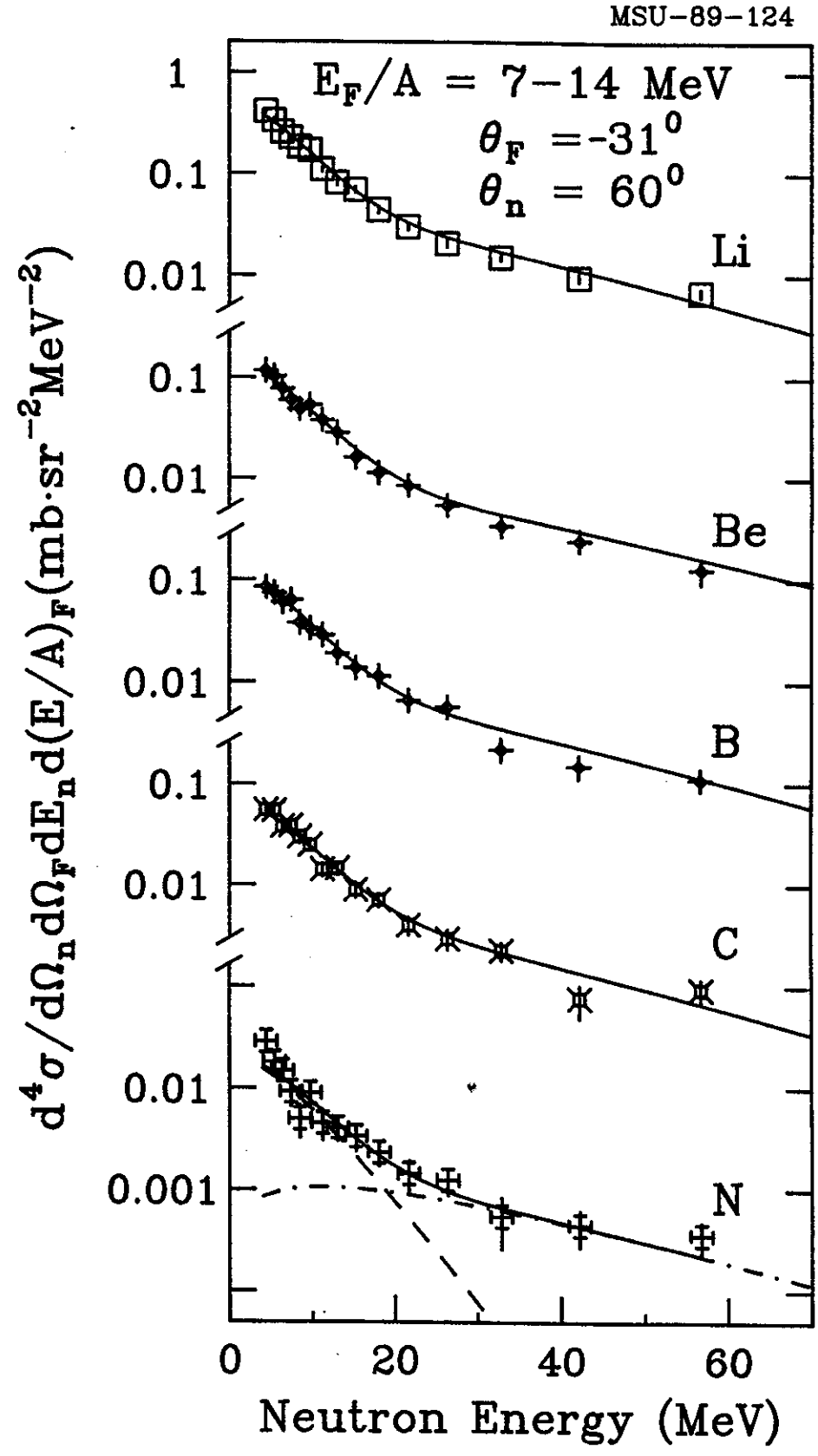
MSU-89-124
E_F/A = 7–14 MeV
θ_F = -31°
θ_n = 60°
Li
Be
B
C
N
1
0.1
0.01
0.001
0
20
40
60
Neutron Energy (MeV)
$d^4\sigma/d\Omega_n d\Omega_F dE_n d(E/A)_F$ (mb·sr^{-2}MeV^{-2})

Fig. 4